Formation of Oxide Phases in the System Fe2O3-Sm2O3

Ristić, Mira; Popović, Stanko; Czako-Nagy, Ilona; Musić, Svetozar

Formation of Oxide Phases
in the System Fe_2O_3–Sm_2O_3

Mira Ristić[1], Stanko Popović[1,2], Ilona Czakó-Nagy[3]
and Svetozar Musić[1]

[1]*Ruđer Bošković Institute, P. O. Box 1016, 41001 Zagreb, Croatia*
[2]*Department of Physics, Faculty of Science, University of Zagreb,*
P. O. Box 162, 41001 Zagreb, Croatia
[3]*Department of Nuclear Chemistry, Eötvös-Lóránd University,*
P. O. Box 32, 1518 Budapest, Hungary

Formation of oxide phases in the system Fe_2O_3–Sm_2O_3 was investigated. The samples were prepared by the solid state reactions at two molar ratios of Fe_2O_3 and Sm_2O_3. The following oxide phases were detected by X-ray diffraction: C-Sm_2O_3, B-Sm_2O_3, α-Fe_2O_3, $SmFeO_3$ and $Sm_3Fe_5O_{12}$. For the molar ratio $Fe_2O_3 : Sm_2O_3 = 1 : 1$, $SmFeO_3$ was detected as one of the oxide phases at temperatures up to 800 °C and as a single phase at 1000 °C and higher temperatures. For the molar ratio $Fe_2O_3 : Sm_2O_3 = 5 : 3$, $SmFeO_3$ was the intermediate phase up to 1200 °C, and $Sm_3Fe_5O_{12}$ was found as a single phase at 1300 °C. The oxide phases containing iron ions were characterized by ^{57}Fe Mössbauer spectroscopy. The formation of $SmFeO_3$ and $Sm_3Fe_5O_{12}$ phases, as end products of the solid state reactions in the system Fe_2O_3–Sm_2O_3, was also investigated by IR spectroscopy.

INTRODUCTION

Rare earth ferrites with perovskite or garnet structures are generally considered to be reaction products between R_2O_3 and Fe_2O_3, R being a rare earth. At high temperatures, R_2O_3 and Fe_2O_3 react to produce rare earth orthoferrite in the reaction:

$$R_2O_3 + Fe_2O_3 \longrightarrow 2RFeO_3 \tag{1}$$

In the presence of additional Fe_2O_3, garnet type ferrite can be also produced at high temperatures:

$$3RFeO_3 + Fe_2O_3 \longrightarrow R_3Fe_5O_{12} \tag{2}$$
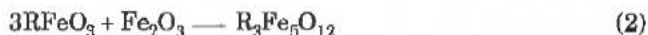
These mixed metal oxides can be prepared in laboratories by the use of different methods. The coprecipitation method involves precipitation of mixed metal hydroxides, $R(OH)_3/Fe(OH)_3$, and thermal treatment of the hydroxide coprecipitate. The sol-gel procedure is very useful for the preparation of oxide particles with a narrow size distribution and defined morphology. However, when two or more metal cations are hydrolyzed simultaneously from their corresponding alkoxides, it is difficult to monitor the particle size distribution and morphology because of different hydrolysis rates of metal cations. Rare earth ferrites with a perovskite or garnet structure can be also prepared by simple thermal decomposition of proper mixtures of inorganic or metal-organic salts, or by pyrolysis of aerosol droplets containing R^{3+} and Fe^{3+} cations. Solid state reactions of the corresponding metal oxides, crystal growth from the melt and film growth on different substrates have been also used to produce mixed metal oxides.

Bachiorrini[1] investigated the synthesis of yttrium iron garnet, $Y_3Fe_5O_{12}$, using the following procedure: a) denitration of the mixture $Y(NO_3)_3 \times 6H_2O + Fe(NO_3) \times 9H_2O$ with organic reducing agents, b) chemical coprecipitation of mixed hydroxides $Y(OH)_3/Fe(OH)_3$, and c) the solid state reaction between Y_2O_3 and Fe_2O_3 at 1300 °C. The reaction products obtained by procedures (a) and (b) crystallized at 730 °C. The best reproducibility of the particle size and morphology was achieved by chemical coprecipitation, as an experimental method.

Kingsley et. al.[2] described the preparation of yttrium aluminium garnet, $Y_3Al_5O_{12}$, by the combustion of a mixture of $Y(NO_3)_3 \times 6H_2O$, $Al(NO_3)_3 \times 9H_2O$ and carbohydrazide, which were previously dissolved in a minimum quantity of water. They also prepared $Y_3Al_5O_{12}$ by the combustion of a mixture of $Y(NO_3)_3 \times 6H_2O$, $Al(NO_3)_3 \times 9H_2O$ and urea. The garnet, $Y_3Al_5O_{12}$, is isostructural with $Y_3Fe_5O_{12}$.

The mixture of Y_2O_3 and Fe_2O_3 with molar ratio 3 : 5 was sintered and heated at a 800 to 1400 °C temperature range for 3 to 12 hours in air.[3] $YFeO_3$ was detected by X-ray diffraction in all samples prepared at temperatures up to 1300 °C. The final product was $Y_3Fe_5O_{12}$. The relative amounts of oxide phases depended on the final temperature of heating and, to a much smaller extent, on the time of heating.

Pyrolysis of aerosol droplets containing metal cations is a relatively simple technique for rapid preparation of mixed metal oxides. This technique[4] was used in the preparation of gadolinium iron garnet, $Gd_3Fe_5O_{12}$. Polydispersed solid spheres of $0.05 - 2$ μm in size were obtained. The $Gd_3Fe_5O_{12}$ yield was $\approx 95\%$ in weight.

Mössbauer spectroscopy found an important application in the characterization of rare earth orthoferrites and garnets.[5] The Mössbauer spectra of the rare earth orthoferrites appeared as far back as in the sixties.[6–10] The Mössbauer spectra of the lantanide orthoferrites show hyperfine magnetic splitting at room temperature. The hyperfine magnetic field, HMF, extrapolated to 0 K, decreases regularly with the atomic number of lantanide cation from 564 kOe for $LaFeO_3$ to 545.5 kOe for $LuFeO_3$.[11]

Michalk and Thiel[12] used Mössbauer spectroscopy to investigate the substitution of Fe^{3+} with Al^{3+} ions in the ytrium iron garnet. $Y_3Fe_{5-x}Al_xO_{12}$, $x = 0$, 0.25 or 0.65. Mössbauer spectroscopy was also used[13] in the study of the double-substituted yttrium iron garnet, $Y_{3-x}Gd_xFe_{5-y}Al_yO_{12}$ ($x = 0.60$ to 1.2, $y = 0.10$ to 0.85).

On the basis of Conversion Electron Mössbauer Spectra (CEMS), Okuda et. al.[14] calculated the HMF values for $Bi_3Fe_5O_{12}$ (421 kOe for 24 d-sites and 491 kOe for 16 a-sites) and for $Y_3Fe_5O_{12}$ (391 kOe for 24 d-sites and 486 kOe for 16 a-sites). Garnet

bubble films, $(Y,Sm,Ca,Tm)_3(Fe,Ge)_5O_{12}$, grown on GGG (gadolinium gallium garnet) substrate and irradiated with 60 keV H_2^+ ions, showed changes in the corresponding CEMS.[15]

The formation of the oxide phases in the system $(1-x)Fe_2O_3 + xGd_2O_3$, $0 \leq x \leq 1$, was investigated by XRD and Mössbauer spectroscopy.[16] The samples were prepared using the chemical coprecipitation procedure. By XRD measurements, the distribution of oxide phases, $\alpha-Fe_2O_3$, $GdFeO_3$, $Gd_3Fe_5O_{12}$ and Gd_2O_3, was determined as a function of x. New accurate crystallographic data for $Gd_3Fe_5O_{12}$ were obtained. The temperatures of the formation of $GdFeO_3$ and $Gd_3Fe_5O_{12}$ were higher in the case of solid state synthesis[17] than in the case of chemical coprecipitation.[16] The formation of oxide phases in an analogous system, $Fe_2O_3-Eu_2O_3$, was also investigated.[18]

Physical properties of garnets, with rare-earth sites fully or partially occupied by Sm^{3+} ions, were previously subjected to several investigations[19,20] because of their possible application in advanced technologies. In this study, we focussed our attention on the formation of oxide phases in the system $Fe_2O_3-Sm_2O_3$. The characteristic properties of the samples were investigated by combined use of X-ray diffraction, [57]Fe Mössbauer spectroscopy and IR spectroscopy.

EXPERIMENTAL

The chemicals were obtained from Ventron. The content of Sm_2O_3 in the starting chemical was determined after its calcination and removal of H_2O and carbonates. Proper weights of oxide powders were mixed and mechanically activated in a planetary mill (Fritsch). The obtained powder was pressed into tablets (Carver press) and heated in air. An LKO II furnace with Kanthal heaters was used for temperatures above 1000 °C. Experimental conditions for the preparation of samples are given in Table I. Two molar ratios, $Fe_2O_3 : Sm_2O_3 = 1 : 1$ and $5 : 3$, were used for the preparation of the $Fe_2O_3-Sm_2O_3$ mixed oxides.

X-ray diffraction (XRD) powder patterns were taken at room temperature using a counter diffractometer with monochromatized Cu $K\alpha$ radiation (Philips diffractometer, proportional counter and graphite monochromator).

The [57]Fe Mössbauer spectra were recorded using a commercial spectrometer (WISSEL). Mathematical deconvolution of the spectra was performed using the SIRIUS program.

All IR spectra were recorded by an IR spectrometer 580B (Perkin-Elmer). The specimens were pressed into discs using spectroscopically pure KBr. The IR spectra are presented as relative transmittance *versus* the wave number (cm^{-1}).

RESULTS AND DISCUSSION

The results of XRD phase analysis of the samples are given in Table II and the crystallographic data for $Sm(OH)_3$, $C-Sm_2O_3$ (body-centered cubic), $B-Sm_2O_3$ (monoclinic), $\alpha-Fe_2O_3$, $SmFeO_3$ and $Sm_3Fe_5O_{12}$ are given in Table III. XRD analysis of the Sm_2O_3, supplied by Ventron, showed that this chemical was actually a mixture of $Sm(OH)_3$ and $B-Sm_2O_3$ (sample S_1). After heating this mixture at 900 °C for 2 hours, a mixture of $B-Sm_2O_3$ and $C-Sm_2O_3$ was obtained (sample S_2), as illustrated in Figure 1. $C-Sm_2O_3$ was also obtained by oxidation of samarium metal in a dynamic *vacuum* at temperatures of 200 to 350 °C. $C-Sm_2O_3$ recrystallized on further heating into crystals of $B-Sm_2O_3$.[21,22]

Heating of a mixture of $Fe_2O_3 : Sm_2O_3 = 1 : 1$ up to 700 °C did not cause formation of samarium orthoferrite, $SmFeO_3$ (samples S_3, S_4 and S_5). Figure 2 shows the characteristic X-ray diffraction powder pattern of sample S_3. $SmFeO_3$ was de-

TABLE I

Experimental conditions of the preparation of samples in the Fe_2O_3-Sm_2O_3 system

Sample	Molar ratio (Fe_2O_3 : Sm_2O_3)	Temperature of heating / °C	Time of heating / hours
S_1	Sm_2O_3, as received by Ventron		
S_2	Sm_2O_3, as received by Ventron	900	2
	1:1	200	1
	1:1	300	1
	1:1	400	1
S_3	1:1	500	24
	1:1	200	1
	1:1	300	1
	1:1	400	1
	1:1	500	1
S_4	1:1	600	5
	1:1	200	1
	1:1	300	1
	1:1	400	1
	1:1	500	1
	1:1	600	1
S_5	1:1	700	5
	1:1	200	1
	1:1	300	1
	1:1	400	1
	1:1	500	1
	1:1	600	1
	1:1	700	1
S_6	1:1	800	5
	1:1	200	1
	1:1	300	1
	1:1	400	1
	1:1	800	5
S_7	1:1	1000	2
S_8	1:1	1200	2
	5:3	200	1
	5:3	300	1
	5:3	400	1
S_9	5:3	800	5
S_{10}	5:3	1000	2
S_{11}	5:3	1100	2
S_{12}	5:3	1200	2
S_{13}	5:3	1300	2

TABLE II

Results of the XRD phase analysis

Sample	Phase composition (approx. molar fractions)	Remarks
S_1	$Sm(OH)_3$ + B–Sm_2O_3	
S_2	B–Sm_2O_3 + C–Sm_2O_3	
S_3	C–Sm_2O_3 + B–Sm_2O_3 + α–Fe_2O_3 (0.30) (0.20) (0.50)	Sharpening of diffraction lines
S_4	C–Sm_2O_3 + B–Sm_2O_3 + α–Fe_2O_3 (0.30) (0.20) (0.50)	
S_5	C–Sm_2O_3 + B–Sm_2O_3 + α–Fe_2O_3 (0.30) (0.20) (0.50)	
S_6	C–Sm_2O_3 + B–Sm_2O_3 + α–Fe_2O_3 + $SmFeO_3$ (0.25) (0.17) (0.43) (0.15)	
S_7	$SmFeO_3$	
S_8	$SmFeO_3$	Sharpening of diffraction lines of $SmFeO_3$
S_9	$SmFeO_3$ + α–Fe_2O_3 (0.05)	
S_{10}	$SmFeO_3$ + α–Fe_2O_3 (0.03)	
S_{11}	$SmFeO_3$ + α–Fe_2O_3 (0.02)	
S_{12}	$Sm_3Fe_5O_{12}$ + $SmFeO_3$ (0.15)	
S_{13}	$Sm_3Fe_5O_{12}$	Sharpening of diffraction lines of $Sm_3Fe_5O_{12}$

Description: C–Sm_2O_3 = cubic, B–Sm_2O_3 = monoclinic

tected as one of the oxide phases in sample S_6, which was produced at 800 °C, and as a single phase at 1000 or 1200 °C (samples S_7 and S_8 respectively). The XRD powder pattern of $SmFeO_3$ produced at 1200 °C is shown in Figure 3. When the mixture Fe_2O_3 : Sm_2O_3 = 5 : 3 was heated to 800 °C, formation of $SmFeO_3$ as the dominant component and of α–Fe_2O_3 as the minor component was detected (sample S_9). With increasing the temperature, the molar content of α–Fe_2O_3 decreased (samples S_{10} and S_{11}). A mixture of $Sm_3Fe_5O_{12}$ and $SmFeO_3$ was generated at 1200 °C (sample S_{12}), and $Sm_3Fe_5O_{12}$ as a single phase (sample S_{13}) at 1300 °C. The XRD powder pattern of $Sm_3Fe_5O_{12}$, produced at 1300 °C, is shown in Figure 4.

The samples containing iron ions were also investigated by ^{57}Fe Mössbauer spectroscopy. The oxide phases α–Fe_2O_3, $SmFeO_3$ and $Sm_3Fe_5O_{12}$, show specific Mössbauer spectroscopic behavior, due to their different structural and magnetic properties.

TABLE III

Crystallographic data* for Sm(OH)₃, C–Sm₂O₃, B–Sm₂O₃,
α–Fe₂O₃, SmFeO₃ and Sm₃Fe₅O₁₂

JCPDS PDF card No	Compound	Space group	Unit cell parameters at 25 °C/nm
6–117[**]	$Sm(OH)_3$	$P6_3/m(176)$	$a = 0.6312,\ c = 0.359$
15–813	$C–Sm_2O_3$	$Ia3(206)$	$a = 1.0927$
25–749[***]	$B–Sm_2O_3$	$C2/m(12)$	$a = 1.418,\ b = 0.3633,$ $c = 0.8847\ \beta = 99.97°$
13–534	$\alpha–Fe_2O_3$	$R3c(167)$	$a = 0.50340,\ c = 1.3752$ (hexagonal axes)
8–149	$SmFeO_3$	$Pbnm(62)$	$a = 0.5394,\ b = 0.5592,$ $c = 0.7711$
23–526	$Sm_3Fe_5O_{12}$	$Ia3d(230)$	$a = 1.2530$

* Source: International Centre for Diffraction Data, Joint Committee on Powder Diffraction Standards, Powder Diffraction File, 1601 Park Lane, Swarthmore, Pa. 19081, USA.

(**) The present work: $a = 0.6375(5),\ c = 0.367(1)$ nm.
(***) The interplanar spacing (d values)) found in this study are approx. 0.3% greater than the ones in card 25–749.

$\alpha–Fe_2O_3$, which possesses the crystal structure of corundum ($\alpha–Al_2O_3$), is characterized by a hyperfine magnetic splitting spectrum (one sextet) at room temperature. The shape of this spectrum depends on the crystallinity of $\alpha–Fe_2O_3$, particle
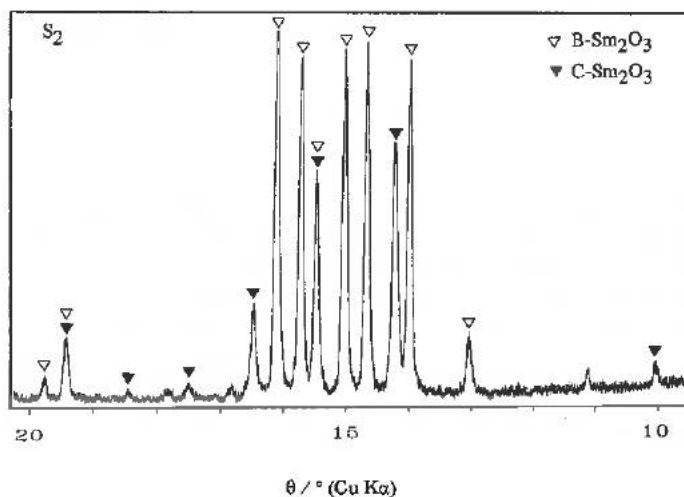

Figure 1. X-ray diffraction powder pattern of sample S_2, recorded at room temperature (∇ B–Sm₂O₃, $\blacktriangledown$ C–Sm₂O₃).
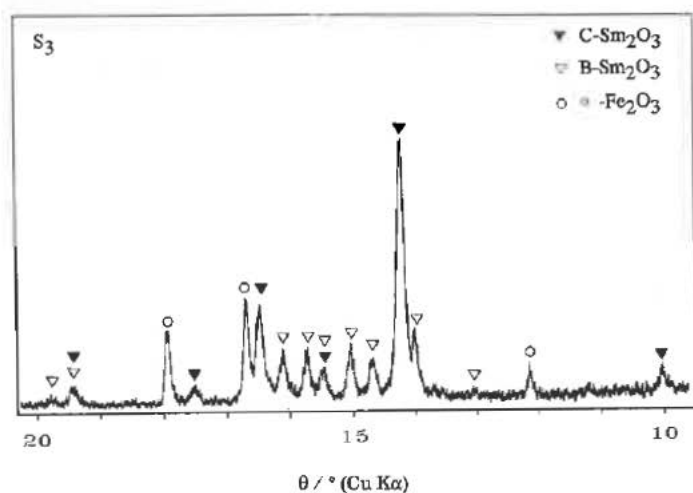
Figure 2. X-ray diffraction powder pattern of sample S_3, recorded at room temperature ($\blacktriangledown$ C–Sm_2O_3, $\triangledown$ B–Sm_2O_3, O α–Fe_2O_3).

sizes and partial substitution of Fe^{3+} ions by other metal ions. Due to these effects, the HMF of α–Fe_2O_3 can be significantly reduced. For instance, in the case of ultrafine α–Fe_2O_3 particles, six spectral lines may collapse into one doublet at room temperature.

The orthoferrites of lanthanide elements possess a distorted perovskite lattice with iron having the same environment throughout the lattice. At room temperature,
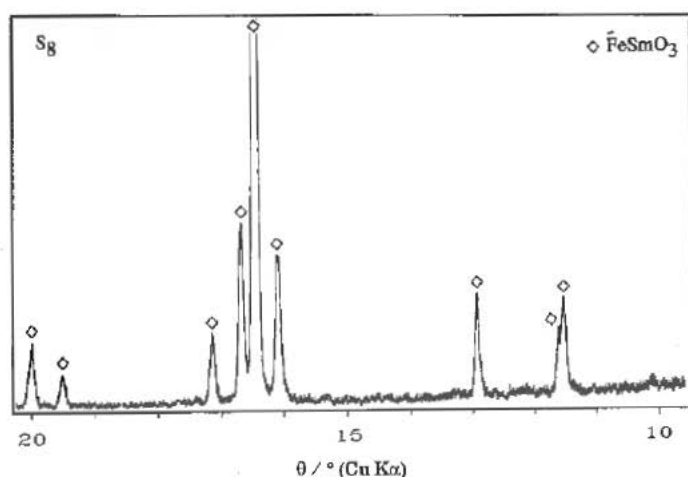
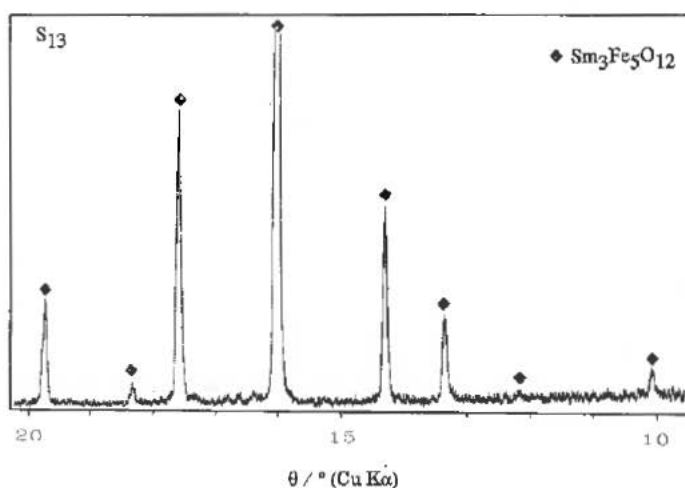Figure 3. X-ray diffraction powder pattern of sample S_8, recorded at room temperature (◊ $SmFeO_3$).

Figure 4. X-ray diffraction pattern of sample S_{13}, recorded at room temperature (♦ $Sm_3Fe_5O_{12}$).

they are characterized by a hyperfine magnetic splitting spectrum. The Mössbauer spectrum of $SmFeO_3$ (sample S_8) is shown in Figure 5. The oxide phases, α-Fe_2O_3 and $RFeO_3$, formed as a result of solid state reactions, may be characterized by similar Mössbauer parameters and, thus, the separation of two subspectra is not visible. For instance, the ^{57}Fe Mössbauer spectra of the mixed oxide phases α-Fe_2O_3-$NdFeO_3$,
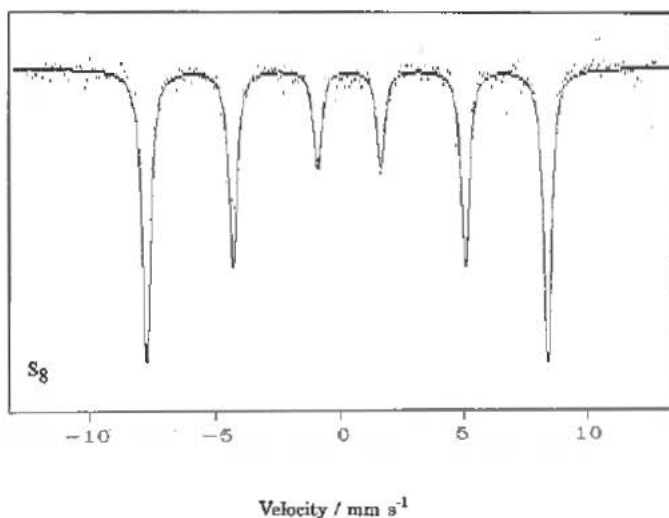

Velocity / mm s⁻¹

Figure 5. ^{57}Fe Mössbauer spectrum of sample S_8, recorded at room temperature, indicating hyperfine magnetic splitting of samarium orthoferrite, $SmFeO_3$.
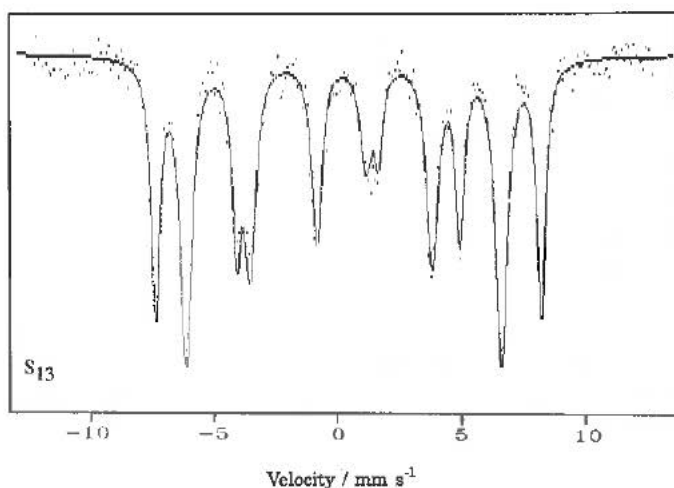
Figure 6. ^{57}Fe Mössbauer spectrum of sample S_{13}, recorded at room temperature, indicating the superposition of two sextets of spectral lines corresponding to iron ions at a- and d-sites with hyperfine magnetic fields of 486 and 398 kOe, respectively.

were found to display one sextet of spectral lines at room temperature.[28] Mathematical deconvolution of these spectra showed distinct regularities in the changes of Mössbauer parameters ΔE_q, Γ and HMF, indicating the presence of two ^{57}Fe subspectra of very similar spectral behavior.

Lanthanide iron garnets, $R_3Fe_5O_{12}$, possess the crystal structure of mineral grossular. Fe^{3+} ions occupy octahedral (a) and tetrahedral (d) sites, while R^{3+} ions are in dodecahedral (c) sites. Figure 6 shows the fitted Mössbauer spectrum of sample S_{13} corresponding to $Sm_3Fe_5O_{12}$. It is characterized by two hyperfine magnetic fields at room temperature, HMF(a) = 486 kOe and HMF(d) = 398 kOe. The ^{57}Fe Mössbauer parameters (RT) calculated for $SmFeO_3$ and $Sm_3Fe_5O_{12}$ are given in Table IV.

TABLE IV

Mössbauer parameters (RT) calculated for $SmFeO_3$ and $Sm_3Fe_5O_{12}$

Compound	Lines	δ_{Fe}/mm s^{-1}	ΔE_q/mm s^{-1}	HMF/kOe
SmFeO₃	M	0.39	−0.07	500
Sm₃Fe₅O₁₂	Ma	0.40	0.08	486
	M$_d$	0.19	0.10	398

Errors: HMF = ± 1 kOe, δ and ΔE_q = ± 0.01 mm/s

The IR spectra of some selected samples are summarized in Figures 7, 8 and 9. The IR spectrum of sample S_6 shows a very strong band at 545 cm^{-1}, pronounced bands at 415, 380 and 350 cm^{-1}, as well as shoulders at 450, 305 and 285 cm^{-1}. With an increase in the temperature of preparation, the very strong band at 545 cm^{-1} (sample S_6) was shifted to 555 cm^{-1} (sample S_8). The IR spectrum of sample S_8, corresponding to SmFeO$_3$, is also characterized by two shoulders at 440 and 415 cm^{-1}, bands at 380 and 350 cm^{-1} and two shoulders at 305 and 285 cm^{-1}.
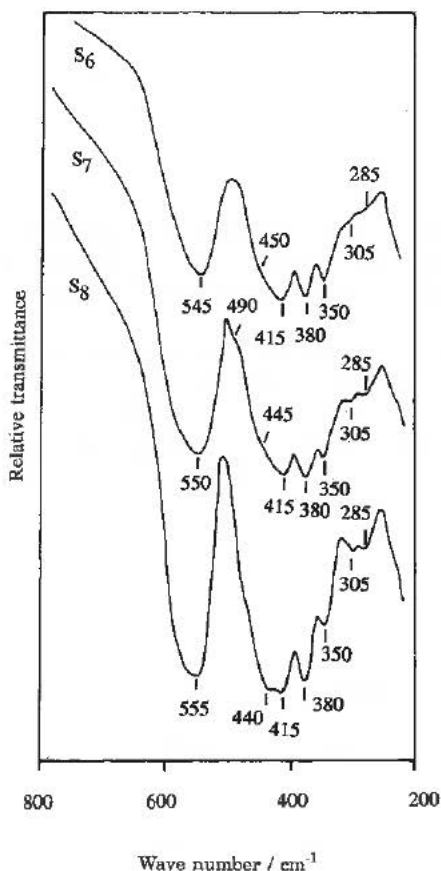

Figure 7. IR spectra of samples S_6, S_7 and S_8, recorded at room temperature.
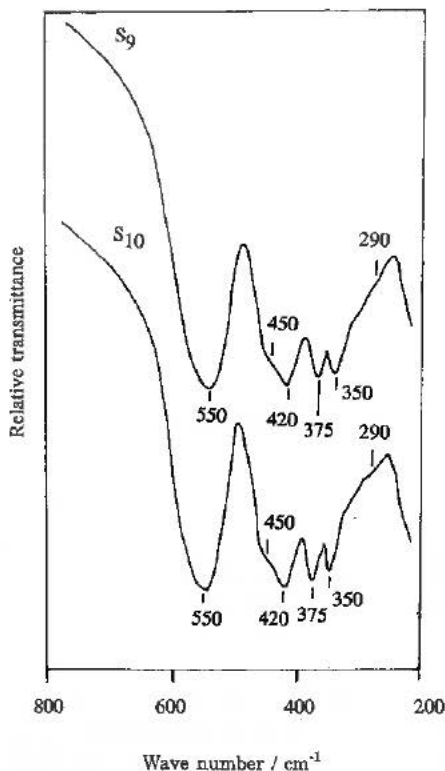

Figure 8. IR spectra of samples S_9 and S_{10}, recorded at room temperature.

Subba Rao *et al.*[24] published the IR spectra of several lanthanide orthoferrites. However, they did not publish the IR spectrum of SmFeO$_3$. They detected a very strong band at 575–543 cm^{-1} for different lanthanide orthoferrites and ascribed it to the Fe–O stretching mode. Significant differences were observed in the region $\simeq$ 450 to $\simeq$ 285 cm^{-1}, due to the nature of lanthanide ions. The present work indicates that the crystal ordering of RFeO$_3$ also affects the corresponding IR spectrum, as illustrated by samples S_7 and S_8.

The specific crystal structure of iron garnets has a strong reflection on their vibrational spectra. In spite of this fact, the changes in the corresponding IR

spectra, during the formation of iron garnets, were not extensively investigated.

Beregi and Hild[25,26] investigated the IR spectra of garnets, $R_3Fe_{5-x}Ga_xO_{12}$, R = Y, Sm, Gd, Er, Yb, Lu, and interpreted them as proposed by Tarte.[27] They assigned a broad and very strong band at $\cong 600$ cm^{-1} to the vibrations of isolated tetrahedra, and a very strong band at $\cong 400$ cm^{-1} to isolated octahedra. They observed a band at $\cong 480$ cm^{-1} in the IR spectra of all rare garnets containing Ga at the octahedral sites ($x > 3$). The intensity of this IR band steadily increased with increasing Ga concentrations.[25,26] In their studies of the vibrational spectra of garnets, $Ln_3Sb_5O_{12}$, Ln = Pr, Nd, Sm, Eu, Gd, Tb, Dy, Ho, Er, Tm, Yb, Botto et al.[28] recorded a strong IR band at 690 cm^{-1} for $Gd_3Sb_5O_{12}$, and ascribed it to the stretching of the shortest Sb–O band, i.e. the Sb(1)–O(1) band. The bands recorded at 602/558 and 460/385 cm^{-1} were discussed in terms of Sb–O–Sb bridge vibrations, and the bands observed below 350 cm^{-1} were ascribed to the SbO₂ bending modes and Ln–O vibrations.

The IR spectrum of sample S₉ is characterized by a very strong band at 550 cm^{-1}, pronounced bands at 420, 375 and 350 cm^{-1}, and shoulders at 450 and 290 cm^{-1}. The IR spectra of samples S₁₀ and S₁₁ are similar to the spectrum of sample S₉. In these samples, SmFeO₃ is the dominant phase. The IR spectra of samples S₁₂ and S₁₃ differ significantly from the previous spectra. The IR spectrum of sample S₁₃, corresponding to $Sm_3Fe_5O_{12}$, is characterized by a very strong IR band having peaks at 630, 580 and 540 cm^{-1}. The second very strong IR band displays a weak band at 420 cm^{-1}, two shoulders at 370 and 355 cm^{-1}, and two shoulders at 320 and 305 cm^{-1}.

Figure 9. IR spectra of samples S₁₁, S₁₂ and S₁₃, recorded at room temperature.

REFERENCES

1. A. Bachiorrini, Silicates Ind. 1990, p. 121.
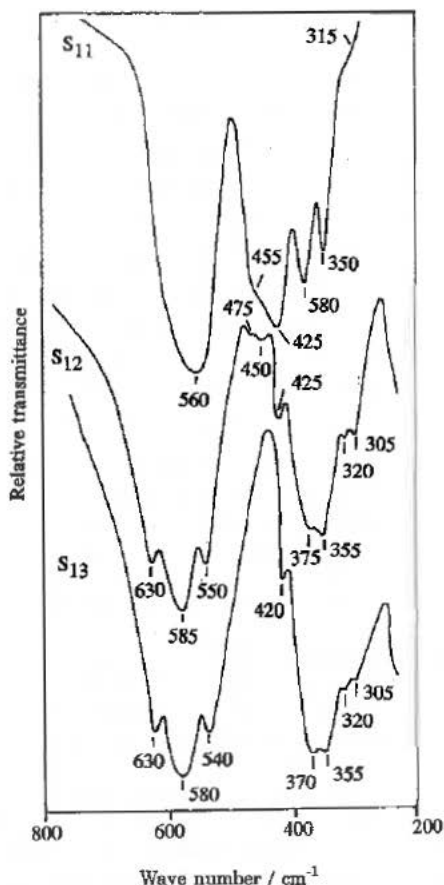2. J. J. Kingsley, K. Suresh, and K. C. Patil, J. Solid St. Chem. 87 (1990) 435.

3. A. Sztaniszláv, E. Sterk, L. Fetter, M. Farkas-Jahnke, and J. Lábár, *J. Magn. Magn. Mater.* **41** (1984) 75.

4. H. K. Xu, C. M. Sorensen, K. J. Klabunde, and G. C. Hadjipanayis, *J. Mater. Res.* **7** (1992) 712.

5. S. Musić, *Mössbauer Spectroscopic Characterization of Mixed Oxides Containing Iron Ions*, in: N. P. Cheremisinoff (Ed.), *Handbook of Ceramics and Composites*, Vol. 2, Chapter 11, M. Dekker Inc., New York–Basel–Hong Kong, 1992, p. 423–463.

6. M. Eibshütz, G. Gorodetsky, S. Shtrikman, and D. Treves, *J. Appl. Phys.* **35** (1964) 1071.

7. D. Treves, *J. Appl. Phys.* **36** (1965) 1033.

8. M. Eibshütz, S. Shtrikman, and D. Treves, *Phys. Rev.* **156** (1967) 562.

9. J. M. D. Coey, G. A. Sawatzky, and A. H. Morrish, *Phys. Rev.* **184** (1969) 334.

10. L. M. Levinson, M. Luban, and S. Shtrikman, *Phys. Rev.* **177** (1969) 864.

11. N. N. Greenwood and T. C. Gibb, *Mössbauer Spectroscopy*, Chapman and Hall, London, 1971.

12. C. Michalk and W. Thiel, *Phys. Stat. Sol.* (a) **90** (1985) 325.

13. D. Barb, L. Diamandescu, R. Puflea, D. Sorescu, and D. Tarina, *Mater. Lett.* **12** (1991) 109.

14. T. Okuda, T. Katayama, H. Kobayashi, N. Kobayashi, K. Satoh, and H. Yamamoto, *J. Appl. Phys.* **67** (1990) 4944.

15. A. H. Morish, P. J. Picone, and N. Saegusa, *J. Magn. Magn. Mater.* **31–34** (1983) 923.

16. S. Musić, V. Ilakovac, M. Ristić, and S. Popović, *J. Mater. Sci.* **27** (1992) 1011.

17. S. Musić, S. Popović I. Czakó-Nagy, and F. Gashi, *J. Mater. Sci. Lett.* **12** (1993) 869.

18. M. Ristić, S. Popović, and S. Musić, *J. Mater. Sci. Lett.* **9** (1990) 872.

19. M. Guillot, H. Le Gall, J. M. Desvignes, and M. Artinian, *J. Appl. Phys.* **70** (1991) 6401.

20. A. H. Rachenfelder, *Magnetic Bubble Technology*, Springer Verlag, Berlin, 1981, cit. in accordance with Ref. 19.

21. C. Boulesteix, P. E. Caro, M. Gasgnier, C. Henry La Blanchetais, B. Pardo, and L. Valiergue, *Acta Crystallogr.* **B26** (1970) 1043.

22. M. Gasgnier, J. Ghys, G. Schiffmacher, C. Henry La Blanchetais, P. E. Caro, C. Boulesteix, C. Loier, and B. Pardo, *J. Less-Common Met.* **34** (1974) 131.

23. S. Musić, S. Popović M. Ristić, and B. Sepiol, *J. Mater. Sci.*, **29** (1994) 1714.

24. G. V. Subba Rao, C. N. R. Rao, and J. R. Ferraro, *Appl. Spectr.* **24** (1970) 436.

25. E. Beregi and E. Hild, *Acta Phys. Hung.* **61** (1987) 235.

26. E. Beregi and E. Hild *Phys. Scr.* **40** (1989) 511.

27. P. Tarte, *Silicates Ind.* **27** (1963) 345.

28. I. L. Botto, E. J. Baran, C. Cascales, I. Rasines, and R. Saez Puche, *J. Phys. Chem. Solids* **52** (1991) 431.